2025 IEEE/SICE International Symposium on System Integration (SII)
January 21-24, 2025, Munich, Germany

Designing Sensor Wear for Posture Estimation with Strain Sensors Using Digital Model

Yumeko Imamura[1], Kunihiro Ogata[1], and Takeshi Kurata[1]

***Abstract*— In this research, we have been developing a wearable motion measurement system for use in remote rehabilitation. A sensor wear with strain sensors is used to measure the motion of the upper limb during rehabilitation movements. Although the measurement target is four degrees of freedom, we aim for highly robust measurements by using 15 strain sensors. However, using actual equipment, it is difficult to find an optimal sensor arrangement by trial and error. Therefore, this study proposes a method for designing sensor placement by analysis, using a digital model that shows human and sensor systems. We designed the sensor wear using measured motions and constructed a model for joint angle estimation by machine learning using long short-term memory (LSTM). We verified the accuracy of the designed sensor wear by simulation.**

I. INTRODUCTION

Elderly people generally face declining muscle strength and joint range of motion due to aging, or limited motor function due to the aftereffects of cerebrovascular disease [1][2]. Rehabilitation is necessary to maintain and improve their quality of life. Improvement of motor function is important for independent living and it also contributes to prevention of falls and maintenance of cognitive function. However, in the recent aging society, the number of elderly people in need of health-care services is increasing, while therapists are in short supply [3]. Transportation services for hospitals and other facilities are insufficient, making it difficult to provide in-person rehabilitation services. In particular, after the COVID-19 pandemic, when travel and face-to-face services need to be avoided, the expectations for remote health-care services are growing. In Japan, the remote implementation of initial interviews to develop health guidance programs has been allowed since 2013, and its diffusion accelerated during the pandemic. The challenge in converting the actual rehabilitation process to a remote one is to maintain the quality of rehabilitation. With an in-person therapist, the user' s movements can be observed from multiple directions and instructions can be provided through physical interaction. When rehabilitation is conducted via video, the observation viewpoint is fixed and the instructions are limited to verbal expression. Therefore, the extent of information exchanged between the user and the therapist is less.

*This work is based on results obtained from a project, JPNP21004, commissioned by the New Energy and Industrial Technology Development Organization (NEDO).

[1]Yumeko Imamura, Kunihiro Ogata, and Takeshi Kurata are with the Human Augmentation Research Center, National Institute of Advanced Industrial Science and Technology (AIST), 6-2-3 Kashiwa-noha, Kashiwa-shi, Chiba, Japan yumeko.imamura, ogata.kunihiro, t.kurata@aist.go.jp

Fig. 1: Concept of an MR^3 device.

We are conducting research and development on rehabilitation training, using virtual reality (VR) and wearable sensing/tactile presentation systems [4]. Although rehabilitation using VR is not common yet, clinical validation shows that it is effective in recovering motor function [5]. However, in tests involving complex movements like assessing the shoulder joint nervous system, the consensus rate of evaluation results among raters is low, diminishing the reliability of the test. A previous study reduced the amount of information by using "full" or "restricted" binary values to evaluate the range of motion to obtain stable results [6]. The exchange of motor and tactile information, in addition to visual and auditory information, is necessary to improve the quality of tele rehabilitation. Accordingly, we are developing devices for this purpose.

In this research project, we are developing a Multimodal mixed Reality for Remote Rehabilitation (MR^3) device equipped with multisensory integration technology to support remote rehabilitation (Fig. 1). Currently, the upper extremity is the target body part. This system consists of MR^3 Wear used by the trainee and MR^3 Mannequin used by the therapist. MR^3 Wear is a garment-type device for measuring the motion of the user's upper limbs [7]. During rehabilitation or functional evaluation, MR^3 Wear measures the trainee's current joint angles and presents it to the therapist, allowing the therapist to understand and evaluate the movement in three dimensions. MR^3 Mannequin is a mannequin with pressure sensors placed on its surface. The therapist touches

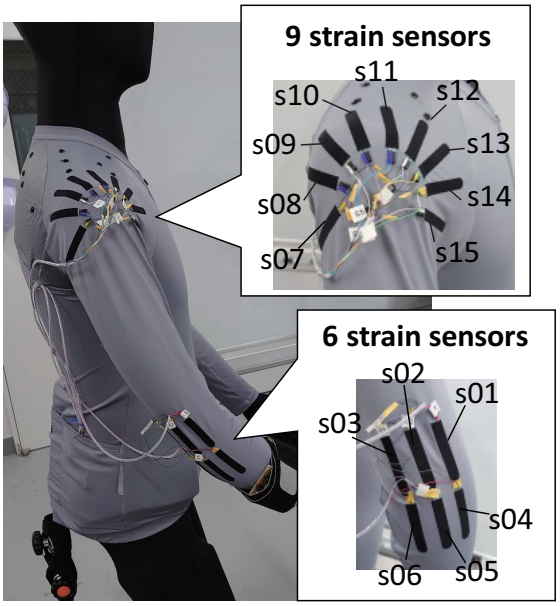

Fig. 2: Prototype of an MR^3 Wear.

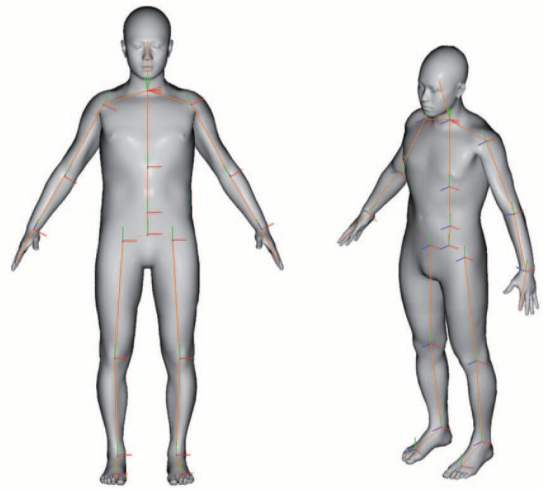

Fig. 3: Human model template [14]. The model consists of a kinematic model and a skin mesh.

the mannequin, considering it a substitute for the trainee to instruct the trainee on the areas to be conscious of. The tactile information received by the mannequin is transferred to the MR^3 Wear and presented to the user through the vibrator embedded in the wear. We also use the pneumatic actuators to induce movement by the hanger reflex phenomenon [8][9]. These technologies are combined to remotely achieve exercise training that is comparable to face-to-face training.

This paper specifically describes the development and analysis of wearable sensing systems for MR^3 Wear. Currently, the predominant method for measuring human posture in wearable devices relies on Inertial Measurement Units (IMUs) [10]. IMUs typically comprise accelerometers, gyroscopes, and magnetometers, which enable the capture of general motion and posture changes in three-dimensional space. However, there is a need for more flexible and comfortable devices suitable for daily use. In response, research has shifted towards flexible strain sensors for posture estimation. These sensors enhance wearability and offer high precision in measuring local deformations. Current studies focus on applying these sensors to specific body parts, such as fingers and hips [11][12]. However, design methodologies for strain-sensor-based posture estimation have yet to be established. Most research relies on empirical methods, making it difficult to accommodate complex movements.

In this research, assuming that rehabilitation is conducted in the daily life environment, we are in the process of developing a motion measurement system using strain sensors. The system does not require environmental preparations such as camera installations. The measurements can be performed by just wearing the system, which maintains the lightness and softness of clothing, and performs robust measurement. Figure 2 shows the prototype of MR^3 Wear. Highly sensitive and low-hysteresis strain sensors [13] are placed around the elbow and shoulder to measure joint motion. Considering that the garment (sensor position) can shift because of the movement or removal of the garment, a redundant number of strain sensors are placed with respect to the degree of freedom (DOF) of the measurement target. Through experiment, we confirmed that it is possible to measure movements that simulate rehabilitation, and in particular, the accuracy of measurement of the elbow joint is high. However, there is still an error in the shoulder joint whose accuracy can be improved by optimizing the sensor placement. Here, producing numerous prototypes with various sensor arrangements on a trial and error basis is a costly operation. This study proposes a method for designing sensor placement by analysis, using a digital model that replicates human and sensor systems. The sensor wear is designed for measured movements and a machine learning model is trained for joint angle estimation. Accuracy verification of the designed sensor wear was conducted through simulation.

II. DIGITAL MODELING

A. Digital human model

In this study, we design an MR^3 Wear in a digital environment, using DhaibaWorks, which is platform software for digital human technology, developed at AIST [14]. The software has a database of Japanese body shapes, a whole-body model template, and can generate individual whole-body models for arbitrary human dimensional values (height, weight, feature point locations, etc.) [15]. The model consists of a 3D triangular mesh representing the human skin surface and a kinematic model with a hierarchical skeletal structure containing 20 links connected by joints. According to the changes in the posture, the skin mesh is deformed by linear blend skinning [16]. Previous studies included the construction of a model to estimate walking motion by inertial measurement unit sensors using DhaibaWorks and the walking motion database [17]. In this study, a virtual

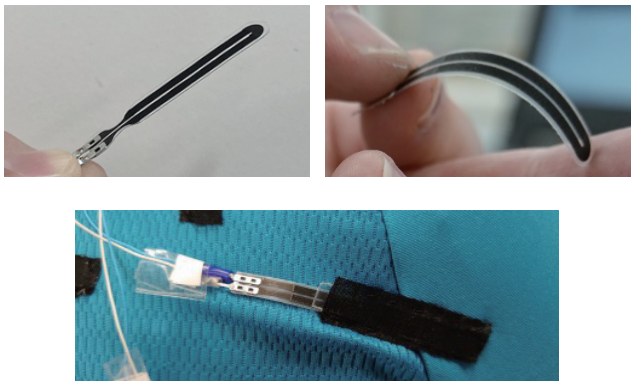

Fig. 4: Appearance of a high-sensitivity strain sensor sheet.

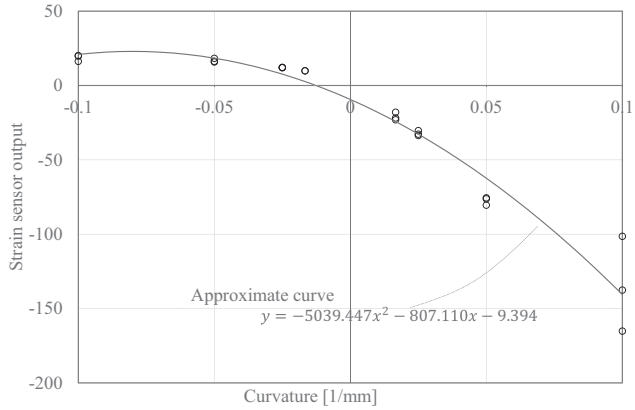

Fig. 5: Strain sensor characteristics. The dots are the measured values. The vertical axis represents the value obtained from AD conversion in 256 levels of 0–3.3V potential. The positive horizontal axis is the front-side bending and the negative is the back-side.

strain sensor element is newly defined and implemented for use in sensor wear analysis.

B. Strain sensor

In this study, we used thin resistive-strain sensors [13]. The sensor is made by printing carbon material on a film to achieve low hysteresis and drift while ensuring a compact and thin structure. Figure 4 shows the appearance of the actual sensor. The sensor can measure both the front and back sides, with a measurement range of up to 0.1[1/mm] curvature for front-side bending and 0.08[1/mm] curvature for back-side bending. Although the sensor can be fabricated to any length, sensors with a length of 45 mm are used for the MR^3 Wear. The relationship between the sensor curvature and the resistance value is shown in Fig. 5.

C. Virtual strain sensor

A virtual strain sensor element is defined to reproduce the strain sensor on the digital human model. The virtual strain sensor represents one sensor with three feature points placed on the surface of the human body model, as shown

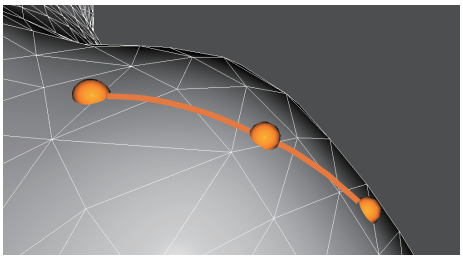

Fig. 6: Virtual strain sensor element.

in Fig. 6. The feature points indicate the two end points and the midpoint of the sensor. The distance between these three points is the length of the sensor, which should be set to satisfy 45 $\pm$ 2 mm when the human model adopts a reference posture. When the joint moves, the shape of the body surface and sensors on the body surface deform, changing the sensor curvature. This curvature is calculated as follows:

- Step 1

Let $\boldsymbol{P}_1$,$\boldsymbol{P}_2$, and $\boldsymbol{P}_3$ be the three feature points representing the virtual strain sensor and $\boldsymbol{C}$ be the center point of the circumscribed circle passing through the three points. A simplified diagram is shown in Fig. 7a. As the distance between $\boldsymbol{C}$ and each feature point is the radius of curvature and its reciprocal is the sensor curvature, the location of the center point $\boldsymbol{C}$ must be determined.

If $\boldsymbol{v}_1 = \boldsymbol{P}_2 - \boldsymbol{P}_1$,$\boldsymbol{v}_2 = \boldsymbol{P}_3 - \boldsymbol{P}_2$, the normal vector of the plane through the three points is

$$\boldsymbol{n} = \frac{\boldsymbol{v}_1 \times \boldsymbol{v}_2}{\|\boldsymbol{v}_1 \times \boldsymbol{v}_2\|}.$$

Vectors $\boldsymbol{u}_1$, $\boldsymbol{u}_2$ perpendicular to the normal vector $\boldsymbol{n}$ and $\boldsymbol{v}_1(\boldsymbol{v}_2)$ are respectively

$$\boldsymbol{u}_1 = \boldsymbol{n} \times \boldsymbol{v}_1, \quad \boldsymbol{u}_2 = \boldsymbol{n} \times \boldsymbol{v}_2,$$

The intersection of a line passing through the midpoint $\boldsymbol{m}_1$ of $\boldsymbol{P}_1$ and $\boldsymbol{P}_2$ and parallel to $\boldsymbol{u}_1$ and a line passing through the midpoint $\boldsymbol{m}_2$ of $\boldsymbol{P}_2$ and $\boldsymbol{P}_3$ and parallel to $\boldsymbol{u}_2$ is the center of the circumscribed circle $\boldsymbol{C}$. The position of $\boldsymbol{C}$ is calculated by determining the coefficients r_1 and r_2 of the following simultaneous equations:

$$\boldsymbol{C} = r_1\boldsymbol{u}_1 + \boldsymbol{m}_1 = r_2\boldsymbol{u}_2 + \boldsymbol{m}_2$$

- Step 2

Furthermore, because strain sensors have different characteristics on the reverse and front sides, it is necessary to determine the direction of sensor bending. Here, the case where the center of the circumscribed circle is inside the body is considered the *front*, and the case where the center of the circumscribed circle is outside the body is considered the *back*. As shown in Fig. 7b, the feature points $\boldsymbol{P}_1$,$\boldsymbol{P}_2$,and $\boldsymbol{P}_3$ are defined on different faces. Let $\boldsymbol{n}_1$,$\boldsymbol{n}_2$,and $\boldsymbol{n}_3$ be the unit vectors of the projection of the normal vectors of these faces onto the plane of the circumscribed circle. Furthermore, let $\boldsymbol{d}_1$,$\boldsymbol{d}_2$,and $\boldsymbol{d}_3$ be the unit vectors in the direction from $\boldsymbol{C}$ to the feature points. Obtain the angles between them.

$$\theta_i = \cos^{-1}(\boldsymbol{d}_i \cdot \boldsymbol{n}_i)$$

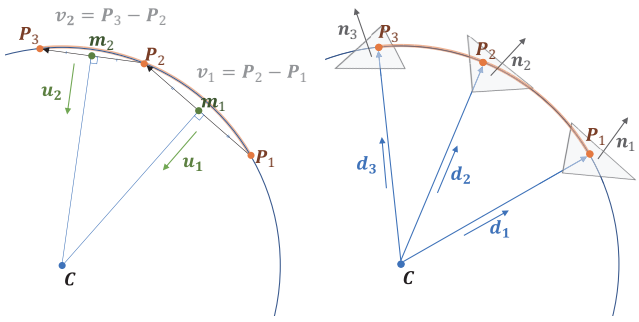

(a) Step 1 (b) Step 2

Fig. 7: Calculation of sensor curvature on the digital human model.

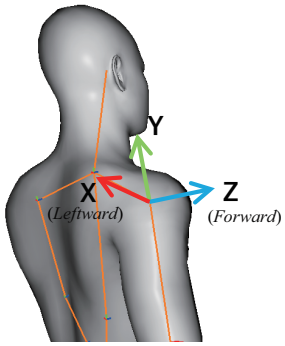

Fig. 8: Definition of the coordinate system of the shoulder joint. The figure shows the posture when naturally arms are lowered and the palms on the thighs.

If two or more θ_i are less than 90 degrees, the sensor is bent in the front direction; otherwise, it is bent in the back direction.

Using the calculated curvature and the regression equation in Fig. 5, the output value of a sensor placed at any position on the body surface, can be estimated.

III. DESIGN OF OPTIMAL SENSOR PLACEMENT

A. Target movement

In this study, postural estimation is performed for rehabilitation and functional evaluation of the upper extremity, especially the shoulder. The target movements were selected as shown in Table I. These movements were measured by an experiment employing three adult male participants. This study received approval from the Life Science Committee of the National Institute of Advanced Industrial Science and Technology (ID: 2022-1247). The target joints are shown in Fig. 8: shoulder 3-axis (X, Y, and Z) and elbow 1-axis (flexion-extension). The motions were obtained by calculating the joint angles from the posture matrix obtained from inertial measurement units (MVN Awinda manufactured by Movella) attached to the forearm, upper arm, and trunk. We aim to estimate the posture of the upper limb in those movements.

TABLE I: List of measured movements

01	Shoulder flexion/extension
02	Shoulder abduction/adduction
03	Shoulder internal rotation/external rotation
04	Elbow flexion/extension
05	Simultaneous flexion of the shoulder and elbow
06	Touching the contralateral shoulder
07	Horizontal shoulder flexion (below 90 degrees)
08	Horizontal shoulder flexion (around 90 degrees)
09	Horizontal shoulder flexion (above 90 degrees)
10	External and internal rotation of the shoulder (with the shoulder abducted and the elbow bent at a right angle)
11	External and internal rotation of the shoulder (with the shoulder flexed and the elbow bent at a right angle)
12	Reaching motion (forward, upward, rightward, leftward)
13	Forward-reaching motion (with a narrow range of motions)
14	Forward-reaching motion (without moving the shoulder blade)
15	Forward-reaching motion (while moving the shoulder blade)
16	Wiping the table in a lateral motion (natural movement)
17	Wiping the table in a lateral motion (reach out as far as possible)
18	Moving the hand from the left knee to the right ear
19	Pulling the arm back and placing the hand on the hip
20	Placing the hand on the back of the head

Motion 01–06 was measured nine times each. Other measurements were performed three times.

B. Optimization method

The optimal sensor arrangement is designed for estimating the upper limb joint angle using a digital human model and virtual strain sensors. The right arm movements are the target of measurement, and the total number of sensors is 15 as in the prototype. The upper limit on the number of sensors was determined by constraints imposed by the actual control board of the device. As the elbow joint is a simple estimation with one DOF, the sensor placement shown in Fig. 9 was chosen to cover the ulnar joint to the radial joint. In the prototype, the elbow joint had a high estimation accuracy, so the number of sensors is reduced to 3, and the remaining 12 sensors are placed around the shoulder joint. Then, the sensor placements for shoulder joint angle estimation are considered. Virtual strain sensors, which are candidates for sensor placement, were stretched over the area around the shoulder joint of the digital human model (Fig. 10). A standard body model of about 170 cm in height was used in this study. The length of the virtual strain sensors was set to 45 mm as described above, with a distance of at least 15 mm between adjacent sensors. The output of these candidate sensors are estimated by simulation, using the measured motion as an input. The sensor placement around the shoulder is selected based on the following evaluation conditions:

- The curvature must not exceed the measurable range of the sensor (-0.08–0.1) during the motion.
- The absolute value of the correlation coefficient between the angle of the joint of interest and the sensor curvature must be 0.7 or greater.

After satisfying the two conditions, the sensors were ranked in order of the range of curvature change during motion. The ranking was applied to each of the three DOFs of the shoulder joint for the motions listed in Table I, and the average ranking was calculated. The four top sensors were selected

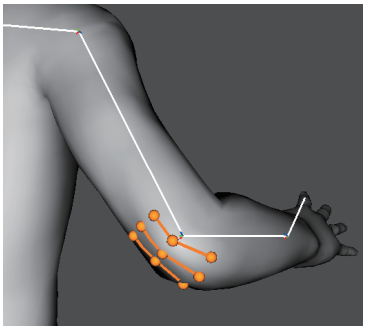

Fig. 9: Sensor position for measurement of the elbow joint.

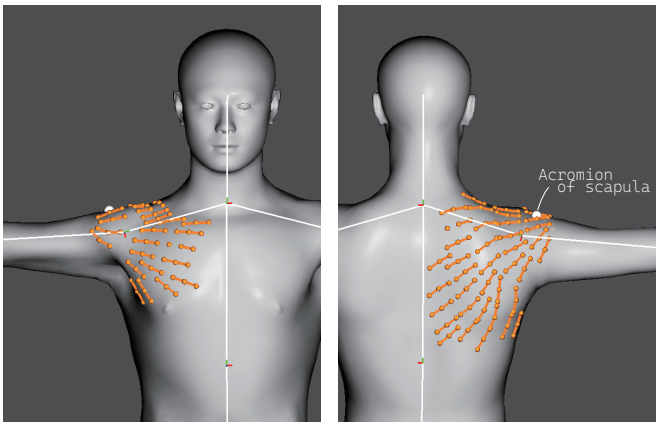

(a) Front view (b) Back view

Fig. 10: Candidate sensor locations for shoulder joint measurement (61 sensor locations).

for each of the three DOFs of the shoulder. The selected sensors are shown in Fig. 11. The sensors on the front of the body were not selected this time. The sensors close to the shoulder joint were sometimes excluded because they would exceed the measurable range. Conversely, the chest sensor was not selected because its deformation during motion was not large. The most significant difference compared with the prototype is that the result indicates that the placement of the sensor on the scapula, especially around the lower edge, may be effective in measuring the joint motion.

C. Machine learning model

Using the sensor placement determined in the previous section, a machine learning model is trained to estimate the joint angle from the sensor output. As the machine learning model, we employed Long Short-Term Memory (LSTM) [18], which is a recurrent neural network widely used in natural language processing and time series data analysis. The model was implemented using Tensorflow 2.10.0. The loss function was set to the mean squared error, the learning rate to 0.001, the minibatch size to 32, the number of epochs to 100, and the optimization algorithm to Adam. The input is the output values of 15 strain sensors for the number of frames set as time-step lengths (e.g., 10 frames is about 150 ms of data). The joint angles of 3 DOFs for the shoulder and 1 DOF for the elbow are estimated.

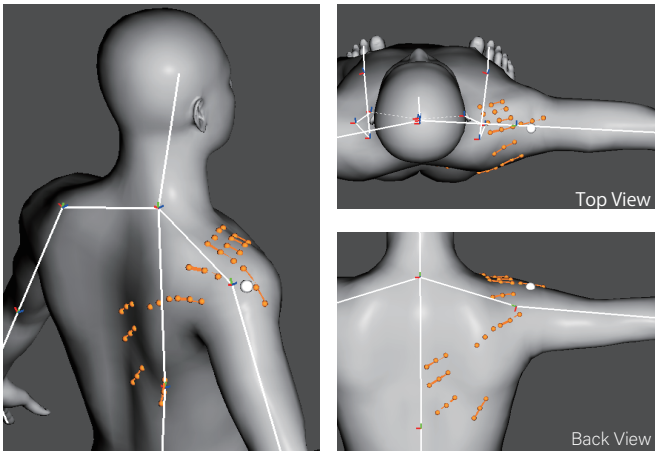

Fig. 11: Strain sensors selected for measurement of the shoulder joint based on the proposed method.

TABLE II: Mean squared error between the input and estimated angles.

		time-step lengths		
		5	10	20
Units	50	0.00397	0.00452	0.00340
	100	0.00340	0.00447	0.00291
	200	0.00419	0.00299	0.00340

The same motion data as described in Section III-A were used to train the model. The data are actual measurements of three participants, each performing the 20 kinds of movements listed in Table I. The movements were measured with a sampling period of approximately 16 msec. Two persons' data were used as the training set, and one person was used as the test set. The measured joint angles were input into the digital human model. The sensor output values during the movements were obtained from the simulation.

Hyperparameters were determined using the grid search method. Three time-step lengths (5, 10, and 20) and three hidden units of LSTM (50, 100, and 200) were set for evaluation. The errors in the joint angle estimation are shown in Table II. From these results, we selected 20 for time-step lengths and 100 for hidden units.

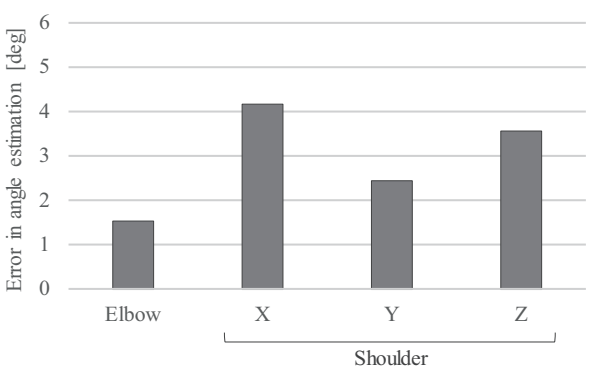

Fig. 12: Joint angle estimation error.

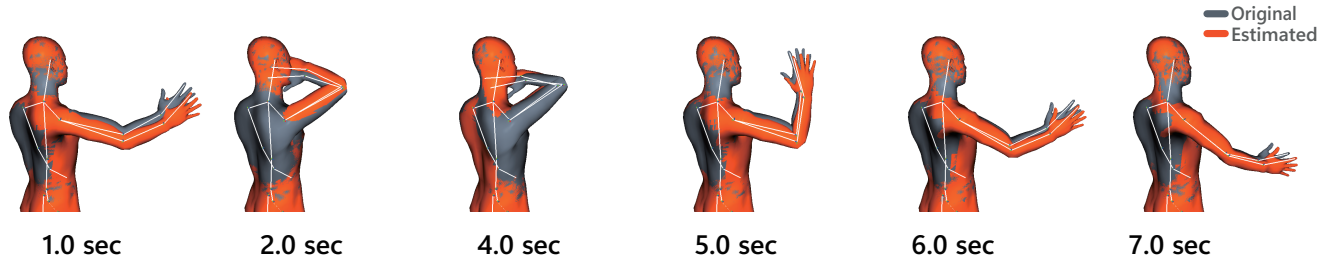

Fig. 13: Original motion and motion estimated from the output values of the virtual strain sensors.

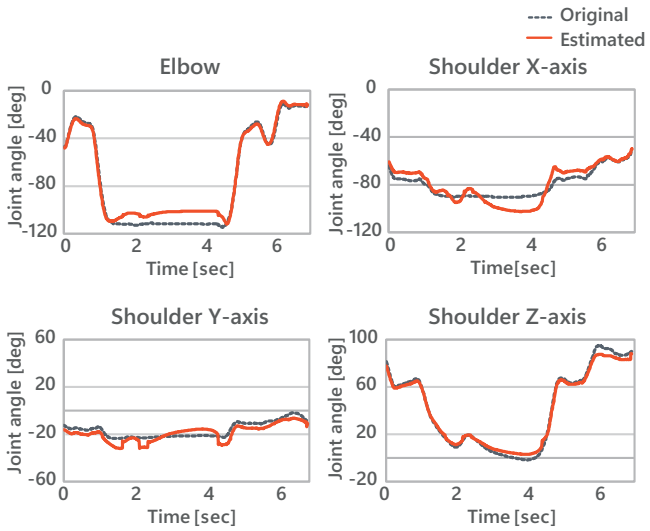

Fig. 14: Comparison of original data and estimated results of joint angles for each axis.

The estimation error resulting from training the model with the above parameters is shown in Fig. 12. The optimized sensor arrangement and LSTM model show that estimation can be performed with an error of less than 5 degrees for all axes. Although the errors for the shoulder X-axis and the Z-axis appear to be relatively large, when normalized by the range of motion of the joint during the target motions, they have approximately the same estimation errors: 1.72%, 1.83%, and 1.60% for the X-, Y-, and Z-axes, respectively. The same number of sensors with high correlations with each axis was selected for sensor selection, which is considered to have evenly increased accuracy. In this research project, the target accuracy on the actual device was set to within an error margin of 15 degrees. It is considered that the designed sensor arrangement can ideally achieve the target accuracy.

D. Validation of posture estimation

The developed estimation model was applied to a motion that was not used for training to verify its usefulness. We used the "Drinking" movement (lifting a drink and holding it close to the face) from the KIT Whole-Body Human Motion Database [19]. Using the feature point positions in the database, inverse kinematics was used to generate the motion for the DhaibaWorks human model. The joint angles of 3 DOFs of the shoulder and 1 DOF of the elbow were used to obtain the output values of the strain sensor by the method described in Section II-C. The joint angle estimation was performed using these values as input to the machine learning model described in Section III-C.

Figure 13 shows the original motion and the estimated motion. Although there are some deviations in the position of the hand depending on the posture, the entire motion is well estimated. The root mean squared errors for each axis is 6.57 degrees, 4.45 degrees, 3.12 degrees and 6.39 degrees, for the shoulder X-, Y-, Z-axes and the elbow, respectively. Time sequence data of joint angles are shown in Fig. 14. Around 1 to 5 seconds on the X-axis, a waveform different from the original data appears. The figure shows that the waveform appearing on the X-axis are similar to those on the Z-axis, which is thought to be affected by the large displacement around the Z-axis. This time, the candidate positions of the strain sensors were determined heuristically and the sensors were selected from them. It may improve the accuracy of motion estimation by making modifications to the sensor positions and directions that can better detect the motion of each axis. In addition, we will also consider exception processing, such as not using a sensor whose value changes rapidly frame-to-frame as an error, and post-processing such as low-pass filtering.

IV. CONCLUSIONS

In this paper, we designed and validated a sensor wear for use in tele rehabilitation, using simulation with digital models. We first defined the digital model of strain sensors using the platform software for digital human technology. We proposed a design method for optimal sensor placement for the target movements and joints. Subsequently, we designed a sensor placement to measure the shoulder joint, using measured motion data. A machine learning model for joint angle estimation was trained by using the joint angle and strain sensor outputs from simulations. The model was verified to be capable of estimating 3 DOFs at the shoulder and 1 DOF with high accuracy using 15 strain sensors. In the future, a prototype will be created based on the design in this paper and the validity will be verified using an actual device.

The digital sensor wear model can enhance estimation accuracy by leveraging publicly available motion capture databases to augment data, simulate individual differences

by generating virtual strain sensor outputs using models of various body sizes, and simulate sensor outputs accounting for shifts in sensor positions during movement. In addition, although this study was limited to the movements of the shoulder and elbow joints, we aim to construct a more useful system by expanding the evaluation of motor functions, such as scapular displacement. We believe that the strain sensor can measure changes in body surface shape in detail, enabling us to evaluate differences in movement that are difficult to quantify using conventional measurement methods such as inertial sensor-based and video-based motion capture. For the purpose, it is necessary to reproduce changes in body surface shape due to displacement of the shoulder blades and the deformation of the garment itself, and the refinement of the digital human model will be an issue for future research.

REFERENCES

[1] Larsson L, Degens H, Li M, Salviati L, Lee YI, Thompson W, Kirkland JL, Sandri M, Sarcopenia: aging-related loss of muscle mass and function, Physiological reviews, vol.99, no.1, pp.427–511, 2019.

[2] Hatem S M, Saussez G, Della Faille M, Prist V, Zhang X, Dispa D, Bleyenheuft Y, Rehabilitation of motor function after stroke: a multiple systematic review focused on techniques to stimulate upper extremity recovery, Frontiers in human neuroscience, vol.10, 442, 2016.

[3] Kinoshita S, Abo M, Okamoto T, Miyamura K, Transitional and long-term care system in Japan and current challenges for stroke patient rehabilitation, Frontiers in Neurology, vol.12, 711470, 2022.

[4] Kurata T, Ogata K, Kanazawa S, Imamura Y, Sato A, Ogiso S, Kobayashi Y, Ichikari R, Nakae S, Tada M, Aoyama T, Shimizu H, Kuzuoka H, Nakamura T, Koshihara T, Kuroda M, Sorimachi H, Oshima K, Project overview on multimodal XR-AI platform for tele-rehab and the reciprocal care coupling with health guidance, TechRxiv, 2023. DOI: 10.36227/techrxiv.24167877.v2

[5] Kim WS, Cho S, Ku J, Kim Y, Lee K, Hwang HJ, Paik NJ, Clinical application of virtual reality for upper limb motor rehabilitation in stroke: review of technologies and clinical evidence, Journal of clinical medicine, vol.9, no.10, 3369, 2020.

[6] Steele L, Lade H, McKenzie S, Russell TG, Assessment and diagnosis of musculoskeletal shoulder disorders over the internet, International Journal of Telemedicine and Applications, vol.2012, 945745, 2012.

[7] Ogata K, Kanazawa S, Tanaka H, Kurata T, Upper Limb Movement Estimation and Function Evaluation of the Shoulder Girdle by Multi-Sensing Flexible Sensor Wear, IEEE/RSJ International Conference on Intelligent Robots and Systems (IROS), pp. 13328–13334, 2022, DOI: 10.1109/IROS47612.2022.9982102.

[8] Asahi T, Nakamura T, Sato M, Kon Y, Kajimoto H, Sato S, The hanger reflex: An inexpensive and non-invasive therapeutic modality for dystonia and neurological disorders, Neurologia medico-chirurgica, vol.60, no.11, pp. 525–530, 2020.

[9] Tanaka K, Nakamura T, Matsumoto K, Kuzuoka H, Effect of Hanger Reflex on detection thresholds for hand redirection during forearm rotation, ACM Symposium on Applied Perception 2023, no.6, pp.1–8, 2023.

[10] Maceira-Elvira P, Popa T, Schmid AC, Hummel FC, Wearable technology in stroke rehabilitation: towards improved diagnosis and treatment of upper-limb motor impairment, Journal of neuroengineering and rehabilitation, vol.16, pp.1–18, 2019.

[11] Jacobs E, Rosen A, Berg-Johansen B, Wang L, Flexible Wearable Nanomaterial-Based Sensing Device for Back Pain and Injury Prevention, IEEE Sensors Letters, vol.7, no.5, pp.1–4, 2023.

[12] Vu LQ, Kim KH, Schulze LJH, Rajulu SL, Lumbar posture assessment with fabric strain sensors, Computers in biology and medicine, vol.118, 103624, 2020.

[13] Kanazawa S, Ushijima H, Development of a strain sensor matrix on mobilized flexible substrate for the imaging of wind pressure distribution, Micromachine, vol.11, no.2, 232, 2020.

[14] Endo Y, Maruyama T, Tada M, DhaibaWorks: a software platform for human-centered cyber-physical systems, International Journal of Automation Technology, vol.17, no.3, pp.292–304, 2023.

[15] Endo Y, Tada M, Mochimaru M, Estimation of Arbitrary Human Models from Anthropometric Dimensions, International Conference on Digital Human Modeling and Applications in Health, Safety, Ergonomics and Risk Management, pp. 3–14, 2015.

[16] Magnenat-Thalmann N, Thalmann D, Human body deformations using joint-dependent local operators and finite-element theory, making them move: mechanics, control, and animation of articulated figures, pp.243–262, 1990.

[17] Kumano Y, Kanoga S, Yamamoto M, Takemura H, Tada M, Estimating Whole-Body Walking Motion from Inertial Measurement Units at Wrist and Heels Using Deep Learning, International Journal of Automation Technology, vol.17, no.3, pp. 217–225, 2023.

[18] Hochreiter S, Schmidhuber J, Long Short-Term Memory, Neural Computation, vol.9, no.8, pp. 1735–1780, 1997, DOI: 10.1162/neco.1997.9.8.1735.

[19] Mandery C, Terlemez Ö, Do M, Vahrenkamp N, Asfour T, Unifying representations and large-scale whole-body motion databases for studying human motion, IEEE Transactions on Robotics, vol.32, no.4, pp.796–809, 2016.